Conformational Flexibility of 1,3-Bis(1-pyrenyl)propane Throughout the Sol−Gel to Xerogel Process

Upvan Narang and Frank V. Bright*

Department of Chemistry, Natural Science and Mathematics Complex, State University of New York at Buffalo, Buffalo, New York 14260-3000

Received January 22, 1996. Revised Manuscript Received April 22, 1996[⊗]

We report on the conformational flexibility of 1,3-bis(1-pyrenyl)propane (BPP) doped within tetramethyl orthosilicate (TMOS)-derived sol−gel materials. In normal liquid solution, at low concentrations ($\sim 10^{-6}$ M), BPP molecules do not form any ground-state dimers; however, on photoexcitation, BPP reorients to form an intramolecular excited-state dimer (excimer). We follow, using steady-state and time-resolved fluorescence spectroscopy, the excimer-like emission from BPP molecules doped within a TMOS-derived sol−gel monolith throughout the entire sol−gel to xerogel formation process. Our results indicate that there are no detectable ground-state dimers formed even after the xerogel has aged and dried for 3 months. In a fresh gel, there is substantial flexibility of the BPP molecules (like in solution) but the flexibility becomes restricted or slowed when the xerogel is formed. We also observe that the conformational flexibility of BPP molecules is reduced further if the solvent is allowed to escape at a faster rate from the sol−gel matrix. As observed in dilute BPP solutions, the fluorescence intensity decay traces for BPP-doped sol−gel-derived glasses at various stages in the sol−gel to xerogel aging process are best described by a triple-exponential decay law. The time-resolved experiments clearly demonstrate that the BPP conformational dynamics are slowed once the xerogel is formed. Together these results provide information on the scale over which dopant dynamics can be controlled within sol−gel-derived composite materials.

Introduction

The sol−gel process is an ambient temperature approach to prepare porous glasses.[1−4] Ambient processing conditions allow one to entrap organic and even bioactive species within these glass matrixes. In addition, one can tune several of the physical characteristics of the final composite (e.g., porosity and surface area) by simply controlling the processing conditions. These features have led to the application of sol−gel-derived materials in fields ranging from chemical sensors[5−15] to nonlinear optics.[16−18]

During the sol−gel process, a liquidlike solution is transformed first into a gel and then, after solvent loss, under ambient temperatures, into a solid glass. These room-temperature-processed glasses are generally termed xerogels. The overall sol−gel process is represented by

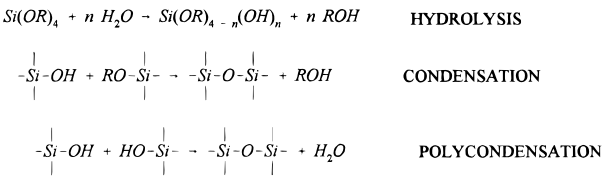

In this simplified scheme, hydrolysis is generally acid or base catalyzed and its rate is highly pH dependent. Temperature, pressure, molar ratio of H_2O, and ROH structure also affect the polymerization process and thus the physicochemical properties of the final glass matrix.[1−4]

Despite the demonstrated applicability of sol−gel-derived materials to a wide range of areas, we continue to lack a complete understanding of the behavior of organic molecules entrapped within a sol−gel-derived

* To whom all correspondence should be sent.

[⊗] Abstract published in *Advance ACS Abstracts,* June 1, 1996.

(1) *Chemical Processing of Advanced Materials*; Hench, L. L., West, J. K., Eds.; Wiley: New York, 1992.
(2) Hench, L. L.; West, J. K. *Chem. Rev.* **1990**, *90*, 33.
(3) Paul, A. *Chemistry of Glasses*, 2nd ed.; Chapman and Hall: New York, 1990; pp 51−85.
(4) Brinker, C. J.; Scherer, G. W. *Sol-Gel Science*; Academic Press: New York, 1989.
(5) Avnir, D.; Braun, S.; Lev, O.; Ottolenghi, M. *SPIE Proc. (Sol-Gel Opt. II)* **1992**, *1758*, 456.
(6) MacCraith, B. D.; McDonagh, C. M.; O'Keeffe, G.; McEvoy, A. K.; Butler, T.; Sheridan F. R. *Sens. Actuat. B* **1995**, *29*, 51.
(7) Rottman, C.; Ottolenghi, M.; Zusman, R.; Lev, O.; Smith, M.; Gong, G.; Kagan, M. L.; Avnir, D. *Mater. Lett.* **1992**, *13*, 293.
(8) Liu, H.-Y.; Switalski, S. C.; Coltrain, B. K.; Merkel, P. B. *Appl. Spectrosc.* **1992**, *46*, 1266.
(9) Zusman, R.; Rottman, C.; Ottolenghi, M.; Avnir, D. *J. Non-Cryst. Solids* **1990**, *122*, 107.
(10) Dunn, B.; Zink, J. I. *J. Mater. Chem.* **1991**, *1*, 903.
(11) Ellerby, L. M.; Nishida, C. R.; Nishida, F.; Yamanaka, S. A.; Dunn, B.; Valentine, J. S.; Zink, J. I. *Science* **1992**, *255*, 1113.
(12) Narang, U.; Gvishi, R.; Bright, F. V.; Prasad, P. N. *J. Sol-Gel Sci. Technol.* **1996**, *6*, 113.
(13) Narang, U.; Prasad, P. N.; Bright, F. V.; Kumar, A.; Kumar, N. D.; Malhotra, B. D.; Kamalasanan, M. N.; Chandra, S. *Chem. Mater.* **1994**, *10*, 1596.
(14) Narang, U.; Prasad, P. N.; Bright, F. V.; Ramanathan, K.; Kumar, N. D.; Malhotra, B. D.; Kamalasanan, M. N.; Chandra, S. *Anal. Chem.* **1994**, *66*, 3139.
(15) Narang, U.; Dunbar, R. A.; Bright, F. V.; Prasad, P. N. *Appl. Spectrosc.* **1993**, *47*, 1700.
(16) Prasad, P. N.; Bright, F. V.; Narang, U.; Wang, R.; Dunbar, R. A.; Jordan, J. D.; Gvishi, R. In *Hybrid Organic-Inorganic Composites*, Mark, J. E.; Lee, C. Y.-C.; Bianconi, P. A., Eds. *ACS Symp. Ser. No. 585*, **1995**, 317.
(17) Prasad, P. N.; Williams, D. J. *Introduction to Nonlinear Optical Effects in Molecules and Polymers*; Wiley: New York, 1991.
(18) Zhang, Y.; Prasad, P. N.; Burzynski, R. *Chem. Mater.* **1992**, *4*, 851.

S0897-4756(96)00040-3 CCC: $12.00

material. Over the past several years, there have been numerous reports on the characterization of sol−gel materials doped with various probe molecules.[18−30] In most cases, the probe molecules were used to better understand the sol−gel process or to investigate the effect(s) of the sol−gel matrix on the actual dopant.

A fundamental issue that has intrigued many sol−gel researchers centers on the conformational dynamics and flexibility of organic molecules/dopants entrapped within sol−gel-derived materials throughout the entire sol−gel to xerogel process and within the final xerogel. Researchers have used several approaches in an effort to address portions of this question. For example, Ilharco et al.[31] doped pyrene-labeled polymers (pyrene attached covalently to one or both ends of a polystyrene chain; MW = 1700 or 5900) within tetraethyl orthosilicate (TEOS)-derived sol−gel monoliths. They investigated the intramolecular pyrene excimer formation during the sol−gel aging process. On the basis of their steady-state fluorescence results, the authors concluded that pyrene dimerization occurs at the beginning of the sol−gel process and the ground-state dimerization/aggregation is enhanced further as the xerogel is formed.

Kaufman et al.[32] probed the pyrene excimer formation within a TMOS-(tetramethyl orthosilicate) and TEOS-derived sol−gel monoliths. High concentrations of pyrene (1 mM) were intentionally doped into the composites to ensure ground-state dimer formation. These investigators observed a strong excimer-like emission in the fresh sol−gel but the excimer emission diminished significantly after the xerogel was formed. These results were explained in terms of a trapping of individual pyrene molecules within isolated sol−gel pores which precluded pyrene−pyrene intermolecular interactions.

Ueda et al.[33] reported on the photochemical behavior of tethered dianthryl compounds in TMOS-derived xerogel monoliths. They reported strong suppression of the intramolecular photodimerization of the dianthryls, suggesting a stearic restriction of the anthryl moieties within the sol−gel matrix. Ueda and coworkers[34] also investigated the cis−trans thermal and photoisomerization of azobenzene within TEOS-derived sol−gel monoliths. In this study, they observed that the sol−gel matrix caused minimal effects on the cis−trans conformational motion of azobenzene.

Fujii et al.[35] reported on the photochromic behavior of 1,2-bis(9-acetoxy-10-anthryl)ethane (AAEA) in TEOS-derived xerogel monoliths which had been aged for 5 months. For this study, sol−gel-based monoliths were prepared using different precursor:water:solvent ratios. The authors showed that, in all cases, AAEA experiences a heterogeneous environment and there is a reduction of the AAEA conformational flexibility within the xerogel matrix.

We recently reported on the rotational reorientation dynamics of rhodamine 6G (R6G) doped within TMOS-derived xerogels.[36] On the basis of steady-state and time-resolved fluorescence anisotropy results, we found that there were two discrete rotational reorientation times for R6G at all stages of the sol−gel to xerogel aging process. These motions were associated with two discrete microdomains within the sol−gel-derived composite. The most interesting aspect of these data was that they showed that the R6G motions are never entirely arrested within the sol−gel composite.

Despite all these studies, there have yet to be any systematic studies on a simple, flexible dopant molecule entrapped within a sol−gel matrix throughout the entire sol−gel to xerogel aging process. In the current work we report on the behavior of the fluorophore, 1,3-bis(1-pyrenyl)propane (BPP), in TMOS-derived sol−gel monoliths. BPP was chosen because (1) its photophysics have been studied extensively, and it is a well-known viscosity probe,[37] (2) it is neutral and less likely to interact strongly with the sol−gel matrix, (3) at dopant loadings (e.g., low micromolar levels) there are generally no intermolecular BPP−BPP interactions, and (4) BPP can fold on itself to form an intramolecular excimer; however, if a static intramolecular ground-state dimer is formed prior to photoexcitation, it can be readily distinguished from the dynamical excimer.

Experimental Section

Materials. The following chemicals were used: TMOS (Aldrich); HCl, Na_2HPO_4, $NaH_2PO_4{\cdot}2H_2O$ (Fisher); ethanol (200 proof; Quantum); 1,3-bis(1-pyrenyl)propane (BPP, Molecular Probes). All reagents were used as received, and aqueous solutions were prepared in double-distilled, deionized water.

Sample Preparation. Sol−gel samples were prepared following the procedure established by Ellerby et al.[11] because this represents one of the more common protocols used to encapsulate organic and bioactive species. A TMOS stock solution was prepared by mixing TMOS, water, ethanol, and HCl in the molar ratio $1:2:2:1.6 \times 10^{-5}$. To prepare an actual sample, we pipeted 1 mL of the stock solution into a standard 1-cm fused silica fluorescence cuvette, added 5 μL of a 300 μM BPP stock solution in ethanol, and then added (with mixing) 0.5 mL of 0.01 M phosphate buffer (pH 7.0). The cuvettes were then covered with parafilm (with and without holes). Throughout the remainder of this paper we refer to the samples with an intact parafilm covering as "sealed cap" samples and those with a perforated parafilm covering as "caps with holes". All samples were prepared in triplicate. All samples were maintained at room temperature (22 ± 1 °C) throughout the entire

(19) Narang, U.; Bright, F. V.; Prasad, P. N. *Appl. Spectrosc.* **1993**, *47*, 229.
(20) Braun, S.; Rappoport, S.; Zusman, R.; Avnir, D.; Ottolenghi, M. *Mater. Lett.* **1990**, *10*, 1.
(21) Avnir, D.; Levy, D.; Reisfeld, R. *J. Phys. Chem.* **1984**, *88*, 5956.
(22) Wang, R.; Narang, U.; Bright, F. V.; Prasad, P. N. *Anal. Chem.* **1993**, *65*, 2671.
(23) Lev, O. *Analusis* **1992**, *20*, 543.
(24) Dunn, B.; Zink, J. I. *J. Mater. Chem.* **1991**, *1*, 903.
(25) Reisfeld, R. *J. Non-Cryst. Solids* **1990**, *121*, 254.
(26) Pouxviel, J. C.; Dunn, B.; Zink, J. I. *J. Phys. Chem.* **1989**, *93*, 2134.
(27) McKiernan, J.; Pouxviel, J. C.; Dunn, B.; Zink, J. I. *J. Phys. Chem.* **1989**, *93*, 2129.
(28) Reisfeld, R.; Chernyak, V.; Eyal, M.; Jorgensen, C. K. *Chem. Phys. Lett.* **1989**, *93*, 2129.
(29) Gvishi, R.; Narang, U.; Bright, F. V.; Prasad, P. N. *Chem. Mater.* **1995**, *7*, 1703.
(30) Narang, U.; Jordan, J. D.; Bright, F. V.; Prasad, P. N. *J. Phys. Chem.* **1994**, *98*, 8101.
(31) Ilharco, L. M.; Santos, A. M.; Silva, M. J.; Matinho, J. M. G. *Langmuir* **1995**, *11*, 2419.
(32) Kaufman, V. R.; Avnir, D. *Langmuir* **1986**, *2*, 717.
(33) Ueda, M.; Kim, H.-B.; Ikeda, T.; Ichimura, K. *J. Mater. Chem.* **1995**, *5*, 889.
(34) Ueda, M.; Kim, H.-B.; Ichimura, K. *Chem. Mater.* **1994**, *6*, 1771.
(35) Fujii, T.; Yamamoto, H.; Oki, K. *J. Mater. Chem.* **1994**, *4*, 635.
(36) Narang, U.; Wang, R.; Prasad, P. N.; Bright, F. V. *J. Phys. Chem.* **1994**, *98*, 17.
(37) (a) Goldenberg, M.; Emert, J.; Morawetz, H. *J. Am. Chem. Soc.* **1978**, *100*, 7171. (b) Zachariasse, K. A.; Duveneck, G.; Busse, R. *J. Am. Chem. Soc.* **1984**, *106*, 1045.

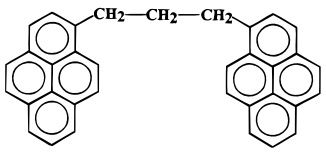

Py — Py

1,3-Bis(1-pyrenyl)propane (BPP)

Figure 1. Molecular structure of the photoprobe BPP.

experiment. After 500 h, the sealed cap samples were unsealed (complete removal of the parafilm cap) to increase the drying rate.

Fluorescence Measurements. All steady-state fluorescence measurements were performed with a SLM 48000 MHF spectrofluorometer using a Xe arc lamp as the excitation source. Emission spectra were background subtracted and corrected for detector and monochromator transmission nonlinearities.

Time-resolved fluorescence data were acquired in the time domain using an IBH 5000 W SAFE time-correlated single-photon-counting fluorometer. The decays were obtained using a N_2 flashlamp operating at 40 kHz as the excitation source (λ_{ex} = 337 nm). In all cases, at least 20 000 counts were acquired in the peak monomer decay channel. Emission was observed through a pair of monchromators (slit width = 8 nm) at 380 and 490 nm. In this configuration the instrument response function and the monomer (380 nm) and excimer (490 nm) decay profiles were acquired simultaneously.

Results and Discussion

Steady-State Fluorescence. In solution, BPP at low concentrations ($\sim 10^{-6}$ M) exclusively forms an intramolecular excimer (i.e., there is no ground-state aggregation).[37b] Previous work has also established that the excimer emission from dilute BPP solutions is a strong function of the local microviscosity surrounding the BPP molecules.[37−43] Specifically, the excimer-to-monomer intensity ratio decreases monotonically (linear at viscosities greater than 10 cp) as viscosity increases.[37−43] In addition, excitation spectra provide direct information on the origin of the excimer emission and the formation of any preformed pyrene−pyrene dimers. Specifically, if any ground-state dimers are formed, emission-wavelength-dependent excitation scans become nonsuperimposable.

Figure 2 presents a series of normalized steady-state fluorescence emission spectra for 1 μM BPP doped within a TMOS-derived sol−gel (seal cap sample) at various times following initial sample preparation. In these particular preparations, the liquid solution gels within 2 min. However, despite the fact that the sol−gel appears to form a macroscopic solid after 2 min, BPP clearly exhibits an excimer-like species (emission at 490 nm) even after 800 h of drying. This result suggests that BPP molecules maintain substantial flexibility when entrapped within the sol−gel matrix, but as the

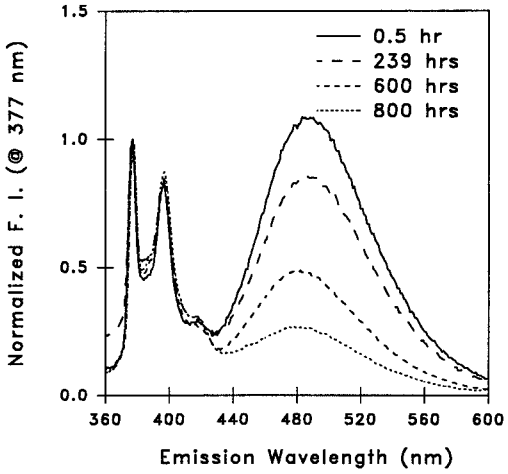

Figure 2. Normalized steady-state fluorescence spectra of 1 μM BPP doped within a TMOS-derived sol−gel during various stages of the sol−gel process.

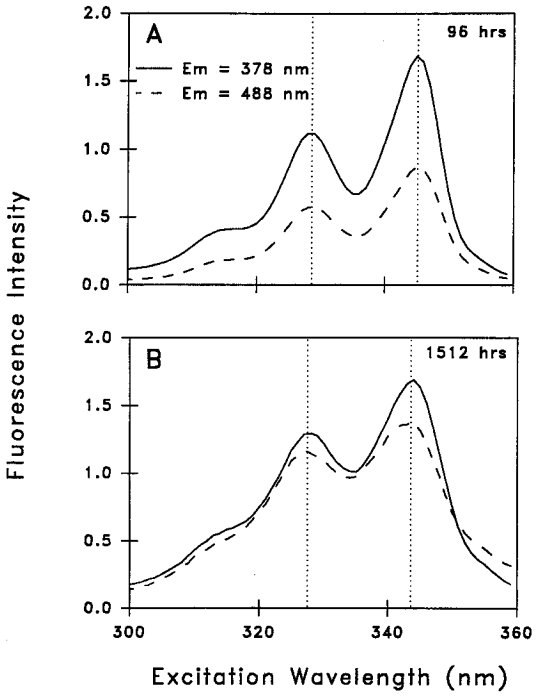

Figure 3. Excitation spectra for 1 μM BPP doped TMOS-derived sol−gel aged under ambient conditions after being aged for 96 h (panel A) and 1512 h (panel B). Solid lines and dashed represent data for emission set at 378 and 488 ± 8 nm, respectively. Excitation bandpass set at 2 nm.

sol−gel ages, the relative extent of excimer-like emission is reduced suggesting a reduction in the flexibility/mobility of the BPP molecules.

To determine if there are any ground-state dimers contributing to the excimer-like emission, we acquired a series of excitation scans at λ_{em} = 378 ± 8 and 488 ± 8 nm for the BPP-doped sol−gels at various stages of the sol−gel to xerogel process. Figure 3 presents typical excitation scans for 1 μM BPP doped in a TMOS-derived sol−gel that has aged 96 (panel A) and 1512 h (panel B). Clearly, individual scan pairs are superimposable, suggesting that there is no detectable ground-state dimerization (inter- or intramolecular) for BPP in the TMOS-derived sol−gel composite during the sol−gel to xerogel transformation. These results are in contrast to a similar study on pyrene-labeled polymers entrapped within TEOS-derived sol−gels[31] where the authors

(38) Rice, J. K.; Christopher, S. J.; Narang, U.; Peifer, W. R.; Bright, F. V. *Analyst* **1994**, *119*, 505.
(39) Yamanaka, T.; Takahashi, Y.; Kitamura, T.; Uchida, K. *J. Lumin.* **1991**, *48* and *49*, 265.
(40) Avnir, D.; Busse, R.; Ottolenghi, M.; Wellner, E.; Zachariasse, K. A. *J. Phys. Chem.* **1985**, *89*, 3521.
(41) Schryver, F. C. D.; Collart, P.; Vandendriessche, J.; Goedeweeck, R.; Swinnen, A.; Auweraer, V. D. *Acc. Chem. Res.* **1987**, *20*, 159.
(42) Zachariasse, K. A.; Duveneck, G.; Kühnle, W. *Chem. Phys. Lett.* **1985**, *113*, 337.
(43) Zachariasse, K. A.; Busse, R.; Duveneck, G.; Kühnle, W. *J. Photochem.* **1985**, *28*, 237.

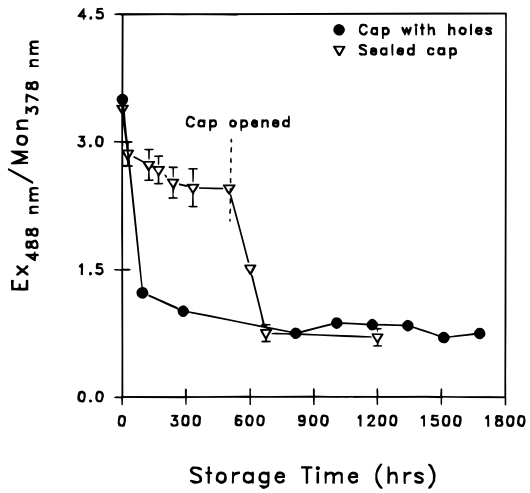

Figure 4. Excimer-to-monomer (Ex/Mon) intensity ratio for 1 μM BPP doped within a TMOS-derived sol−gel as a function of storage time. Symbolism: Samples aged under ambient conditions with sealed cap (▽) and cap with holes (●).

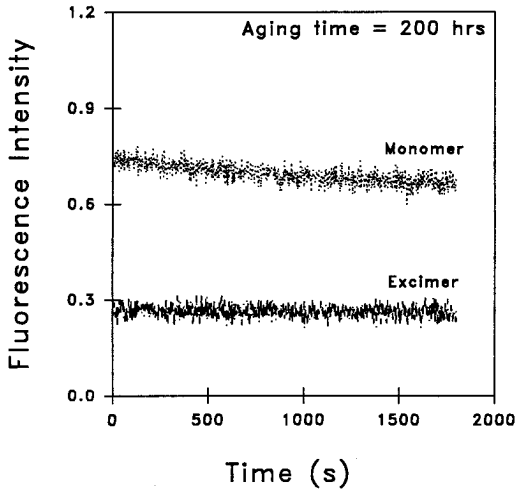

Figure 5. Slow-time acquisition of the fluorescence at 370 ± 8 nm (monomer) and 490 ± 8 nm for a 1 μM BPP doped TMOS-derived sol−gel aged for 200 h under ambient conditions. λ_{ex} = 325 nm.

observed nonsuperimposable emission-wavelength-dependent excitation scans caused by ground-state pyrene aggregation in the beginning of the sol−gel process. This was not surprising because the pyrene-labeled polymers doped within the sol−gels varied from 1700 to 5900 in MW with a reported radius of gyration of ~11.8 Å. On the basis of N_2 adsorption isotherms, the average radius of the pores within those xerogels was 10 Å. Therefore, because the entrapped molecules are larger than the average xerogel pore size, intramolecular pyrene aggregation of the pyrene-labeled polymers was expected. In the current work, we have entrapped a much smaller molecule (BPP) and observe far greater flexibility within the sol−gel pores and no ground-state aggregation throughout the sol−gel to xerogel process.

Figure 4 presents the change in the excimer-to-monomer (Ex/Mon) intensity ratio of BPP-doped within a TMOS-derived sol−gel as a function of storage time. Data were collected for two sets of triplicate samples, one stored with completely sealed caps (▽) and the other with holes in the caps (●). In both the cases, the Ex/Mon ratio before buffer addition is 2.2. In pure ethanol, the Ex/Mon ratio under similar experimental conditions was 2.1 (in good agreement with the previously published results).[37b] Upon addition of the buffer (gelation can occur within 2 min for the uncapped samples) the Ex/Mon ratio increases to ~3.4. This result most likely arises because the aqueous buffer serves initially to lower the overall system viscosity prior to actual gelation of the solution. Excitation scans (not shown) rule out any form of ground-state preassociation and any sort of anomalous photoinstability of the BPP under our experimental conditions is dismissed (Figure 5).

Time-Resolved Fluorescence

The static fluorescence strongly suggests that the sol−gel-entrapped BPP molecules are able to form an excimer within the sol−gel composite. Figure 6 presents a series of time-resolved intensity decay traces for BPP in the TMOS-derived sol−gel samples aged 315 and 1345 h. (Note: The samples were purged with N_2 to remove O_2.) In panel A is shown the instrument

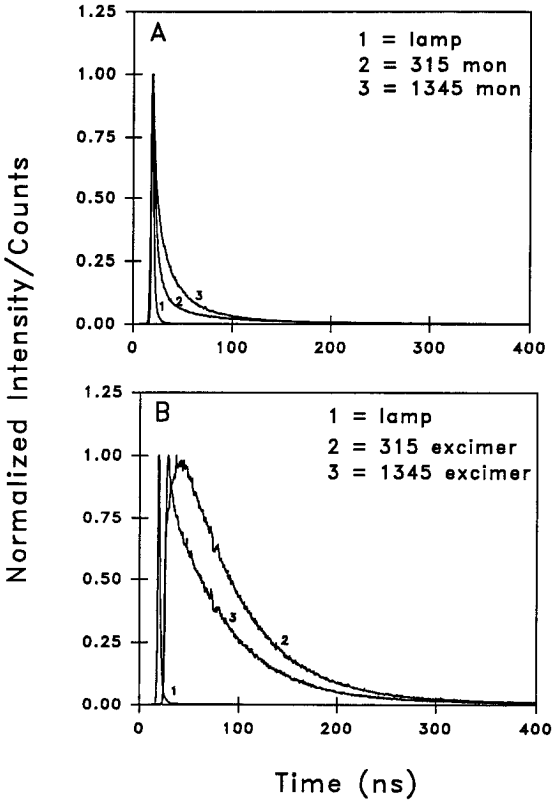

Figure 6. Normalized excited-state decay traces for 1 μM BPP doped TMOS-derived sol−gel when excited at 337 nm. The decay curves were collected at 390 + 16 nm (panel A) and 490 + 16 nm (panel B). Decay curves 1, 2, and 3 correspond to the lamp response, 315 h of aging time, and 1345 h of aging time for the BPP−sol−gel sample, respectively.

response function (trace 1) and the decay traces associated with the *monomer* emission (380 nm) for the 315 (trace 2) and 1345 h old (trace 3) samples. Similarly, panel B presents the instrument response function (trace 1) and the decay traces for the *excimer* emission (490 nm) for the 315 (trace 2) and 1345 h old (trace 3) samples. Table 1 summarizes the results of these experiments. Inspection of these results reveals several interesting features. First, like BPP in liquids, the decay kinetics can be reasonably well modeled by a three-component decay law. Second, the classical ex-

Table 1. Decay Times for 1 μM BPP Doped in a TMOS-Derived Sol−Gel Monolith after 315 and 1345 h

sample	decay model	τ_1;[a] (F_1)[b]	τ_2;[a] (F_2)[b]	τ_3;[a] (F_3)[b]	(χ^2)[c]
BPP 315 h, monomer	single	11.8			196.0
	double	3.42 (54)	71.9 (46)		25.0
	triple	1.51 (38)	16.0 (30)	119.8 (32)	2.8
BPP 315 h, excimer	single	65.2			19.0
	double	4.1 (40)	62.4 (60)		8.4
	triple	1.0 (1.6)	7.2 (−7.6)	61.7 (106)	2.4
BPP 1345 h, monomer	single	24			83
	double	7.3 (46)	49.1 (54)		17.3
	triple	2.3 (22)	21.1 (54)	90.8 (24)	2.5
BPP 1345 h, excimer	single	28			47
	double	8 (18)	76 (82)		10.5
	triple	2.6 (3)	55.6 (11)	165 (86)	1.4

[a] τ is the excited-state decay times in nanoseconds. [b] F_i is the fractonal contribution (percent) of the respective excited-state lifetime, τ_i. [c] In general χ^2 values for the triple-exponential decay fits are not unity; however, residuals and autocorrelation traces (not shown) are reasonably random.

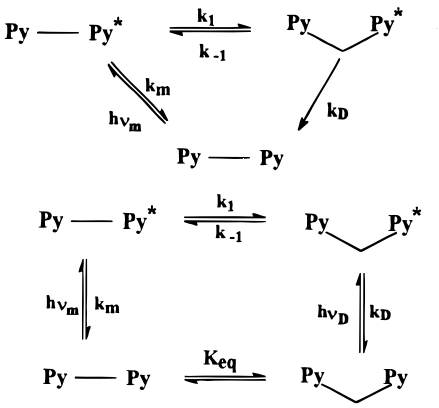

Figure 7. Energy-level diagrams for BPP. (Upper panel) The energy-level diagram for BPP in liquids and the TMOS-derived sol−gels. Symbols: Py−Py, Py−Py*, PyVPy*, $h\nu_m$, k_m, k_1, k_{-1}, and k_d represent the ground-state BPP that is not preassociated, locally excited BP before it folds, excited-state BPP that has folded to form the excimer, absorbance by the monomer, monomer deexcitation rate, unimolecular rate for excimer formation, unimolecular rate for excimer dissociation, and dimer deexcitation, respectively. (Lower panel) The energy-level diagram proposed when ground-sate aggregation of BPP takes place. Symbols: PyVPy, $h\nu_d$, and K_{eq} represent the ground-state BPP folded such that the two pyrenes are preassociated, absorbance by the preassociated dimer, and the equilibrium constant between the ground-state BPP monomer and dimer, respectively (all other symbols are the same as defined in the upper panel).

cimer "growing in" is seen clearly for the 315 h old sample at 490 nm (curve 2 in panel B). Third, the intensity decay profiles for the monomer and excimer emission are completely different from one another (compare panels A and B), and this is fully consistent with the behavior of BPP in liquids.[37−43] Finally, our measured decay times (Table 1) are in good agreement with values recovered for BPP in other media.[37−43]

Conclusions

We report on the behavior of the flexible photoprobe BPP in TMOS-derived sol−gel throughout the sol−gel to xerogel formation process. There is no interaction between the BPP probes and there is no evidence for inter- or intramolecular ground-state dimerization. Thus, the basic mechanism of the BPP dynamics in the sol−gel glass is described by the upper panel in Figure 7. The lower panel, suggestive of ground-state dimer formation, does not appear to describe the BPP photophysics in the TMOS sol−gel matrix. As the sol−gel ages, the flexibility of the BPP molecule is slowed or hindered and k_1 (see Figure 7) decreases as the xerogel forms and ages. However, throughout the aging process the intramolecular excimer formation process is *not* arrested completely. Together these results demonstrate that the size of the dopant as well as its flexibility dictate the extent to which the dopant dynamics are affected by the sol−gel composite.[44]

Acknowledgment. This work was generously supported by the National Science Foundation (CHE-9300694).

Note added in proof: During the time between when this paper was accepted and galley proofs arrived, a paper (Kweon, M.; Lee, Y. H.; Ahn, B. T.; Lee, U. *Bull. Korean Chem. Soc.* **1996**, *17*, 158) appeared wherein the authors reported on the photophysics of BPP in TEOS-derived sol−gels.

CM960040V

(44) Jordan, J. D.; Dunbar, R. A.; Bright, F. V. *Anal. Chem.* **1995**, *67*, 2436.